

Numerical Simulation and Experimental Study of Thermal Distribution Behavior in Downdraft Ceramic Kiln

Chartchai Dechpratoom¹, Arpiruk Hokpunna², Pracha Yeunyongkul¹, Ronnachart Munsin¹
Thanawat Watcharadumrongsak¹, Korawat Wuttikid^{1*}

¹Mechanical Engineering Department, Faculty of Engineering,
Rajamangala University of Technology Lanna Chiang Mai, Chiang Mai, Thailand

² Mechanical Engineering Department, Faculty of Engineering,
Chiang Mai University, Chiang Mai, Thailand

*Corresponding author. Email: korrawat_wuttikid@rmutl.ac.th

ARTICLE INFO

Received: 30/04/2023
Revised: 15/06/2023
Accepted: 08/08/2023
Published: 28/08/2023

KEYWORDS

Downdraft kiln;
Stoneware ceramic;
Thermal distribution;
CFD model;
Thermocouple.

ABSTRACT

This research aims to study and analyze thermal distribution behavior in 3.6 m³ downdraft kiln containing standard 10 layers and 250 kg ceramic shelf. This understanding is expected to solve the waste product problem of stoneware ceramic affected by uneven inside temperature. Thermal distribution was analyzed by thermocouple measuring simultaneously CFD method. Regularly, R - type thermocouples measurements were permanently installed for 8 points around the kiln, front middle and rear top, door, mid - rear wall, side wall, chimney and burner. These measuring results compared to CFD show the trend. The temperature on the top kiln was higher than that bottom. The average temperature on the top kiln was around 1,160°C whereas that on the bottom kiln was around 850°C. The CFD results were error from thermocouple measuring for -2 to 5%. However, CFD results also show thermal distribution behavior at the immeasurable point from thermocouple. The temperature distribution on the bottom kiln was uneven. The temperature nearby the front kiln was slightly lower than that rear kiln because the outlet vent to the chimney is near rear kiln.

Doi: <https://doi.org/10.54644/jte.78B.2023.1440>

Copyright © JTE. This is an open access article distributed under the terms and conditions of the [Creative Commons Attribution-NonCommercial 4.0 International License](https://creativecommons.org/licenses/by-nc/4.0/) which permits unrestricted use, distribution, and reproduction in any medium for non-commercial purpose, provided the original work is properly cited.

1. Introduction

Precise control of temperature, time and atmospheric firing in each firing period are key factors affecting the pottery quality, suitable hardness, consistency shrinkage and product size. This also causes the clay body and glaze being vitrified. The uniform temperature distribution inside the kiln is one key factor affecting the capability of firing process in contrast uneven distribution increases the risk of malformations and breakage of ceramic pieces. Naturally, the temperature in the downdraft ceramic kiln at top area is higher than that the bottom area causing incomplete firing products (defected product) at bottom kiln. To avoid this problem, some low materials are avoided putting at bottom kiln. It means loss of opportunity about 10% to utilize the kiln volume. Normally, precise temperature controlling depends on number of thermocouple sensors around inside kiln. But practically, thermocouples cannot be installed every required point inside kiln. Because their high cost and they can obstruct arrangement of workpiece or kiln car. Presently, Computational Fluid Dynamics (CFD) technique is widely used to simulate the temperature behavior inside the kiln while the firing process or soaking fire. CFD can display the temperature distribution on some positions uninstalling the measuring device. Reliability of CFD result is usually compared with actual measuring tool. This is also beneficial to reduces the risk of new investment building and testing in various conditions. Reliable CFD can be predicted the required results from varying input parameters (air or fuel flow rate, inside kiln part adjustments, gas pressure, etc.) for future development. The examples for CFD utilization are following. T. Fongsamoot, et al proved CFD reliability by comparing to experiment result. The model was solved by conservation equation for mass, momentum and energy together with the k-ε turbulent model. Input variable for simulation were adjusting the width of the hot-fluid baffle as half of the chimney and stepwise increasing gas pressure from 20 to 70 kPa in 1 m³ kiln. The results show the firing reduction time up to 75 minutes

(16%) and fuel reduction by 17%. T. S. Possamai, et al. 0 presented a thermal energy transport model in ceramic frits melting kilns with oxy-firing combustion process working in temperature of 1400 °C. The purpose is to reduce the energy consumption in particular type of kiln without a production reduction. The model estimated the values influenced from varied variables of kiln geometry, burner position, fuel, and oxidizing format. Then, providing the suitable data to completely approach problem solving involving real kiln structure improvement. The CFD and experimental data were consistent with the real phenomena. Z. Zhang, et al, 0 applied CFD to the sintering process in the trial production of household porcelain. They can improve burner flame velocity for uniformity of kiln temperature. K. Krumov, et al, 0 developed the algorithm for numerical analysis of the transient thermal processes for ceramic firing. This development can analyst kiln efficiency. K. S. Krumov, et al, 0. used CFD model checking the heat flow format in the combustion chamber causing the waste problem. they mentioned method analyzing the heat transfer in the ceramic kiln to provide high temperature and efficiency. The suggestions for combustion equipment improvement, rearrangement of chamber space is expected to achieve reduce heat losses, well heat transfer, high efficiency of energy consumption, productivity and waste reduction. M. Romero-Flores, et al 0 used CFD to investigate the temperature distribution in a sanitary ware kiln. It was found that the burners were installed too close each other resulting in poor temperature distribution due to airflow collisions. To avoid this effect, relocation between hot gases exhaust and burners was suggested. U. Adhikari, et al, 0 observed firing behavior in pottery kilns (temperature distribution, flame temperature) by CFD. Then, recommendation of optimum modification of existing kiln can improve specific fuel consumption of different kiln from 234 kcal/kg to 573 kcal/kg. According to the researches, CFD was utilized to investigate and improve firing behavior inside the kiln from different concepts and jobsite depending on point of view of each research. This work also presents another aspect holding the same goals as the previous research to study and analyze thermal behavior of the temperature distribution in a downdraft ceramic kiln. In this work, to confirm reliability of CFD result, not only the temperature measurement from thermocouple but also Pyrometric device 0 is used to check temperature equivalent form the product shrinkage after firing by related data of temperature and time. The reports of standard deviation of shrinkage distortion can check capability of firing process and are applied to adjust workpieces arrangement util acceptable criteria or reproducibility. These are not a temperature value but it's "sintering intensity" 0.

2. Materials and Methods

2.1. Theory and Research Method

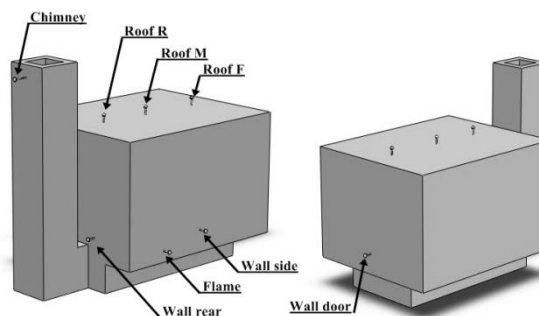


Figure 1. *Temperature measurement positions*

Downdraft ceramic kiln having volume of 3.65 m³ for glaze firing by LPG fuel was used as a prototype in this work (Figure 1). It contains 10 shelves for placing the underglaze hand-painted stoneware tableware. The ceramic fiber insulator was installed whole inside wall kiln. In general, traditional ceramic firing cycle includes the step of heating (heating up kiln temperature from ambient to ~800°C), firing (~800°C to peak temperature) and soaking (being constant peak temperature 10-30 minutes), respectively. 0. Soaking step makes all items completely burnt throughout the kiln. It is the condition for studying in this work. During this period, the flow rate of the fuel is quite constant before stopping fuel supply. The temperature distribution inside the kiln is between 1,100 to 1,200°C. The temperature inside the kiln was recorded and measured by using data logger and R-type thermocouples

installed at 8 positions as shown in Figure 1. Roof F, Roof M and Roof R indicate Front, Middle and rear Roof, respectively. Inclined Manometer was used along with S-Pilot tube to measure the different pressure from atmosphere in chimney according to US.EPA Method 0.

Pyrometric devices, Process Temperature Control Rings (PTCR ring) type LTH (application range of 970-1250°C) were used to measure the dispersion. There are 4-point PTCR rings placed inside the kiln as shown in Figure 2.



Figure 2. Arrangement of workpieces and PTCR ring on the shelf

2.2. Model and Assumption

The 3D model was created from the actual scale of the kiln in use as displayed in Figure 3. The chamber size is $1.76 \times 2.35 \times 1.56 \text{ m}^3$ (width \times length \times height). The chimney has 0.24 length m. hydraulic. Due to symmetry of kiln shape, the model domain was built only as half kiln. The grids independence was verified by gradually increasing the number of grids during from 300,000-6,500,000 cells until the required results were not much changed. Ansys Fluent program was applied to analyze the result of created model. The assumptions in the calculation are Steady State. There is no slippage on the wall surface and adiabatic walls. The hot air with constant density was working fluid. The flow of air inside the kiln was turbulent flow according to Standard k- ϵ . The constant to cover a wide range of turbulent flow was set as following: $C_\mu = 0.09$, $\sigma_k = 1.00$, $\sigma_\epsilon = 1.3$, $C_{1\epsilon} = 1.44$, $C_{2\epsilon} = 1.92$. The boundary conditions for this simulation are detailed in Table 3 as follows. The actual temperature and the hot air volume flowrate leaving from the kiln were used as inputs for the CFD program.

$$\underbrace{\frac{\partial(u\Phi)}{\partial x} + \frac{\partial(v\Phi)}{\partial y} + \frac{\partial(w\Phi)}{\partial z}}_{\text{advection}} = \underbrace{\frac{\partial}{\partial x} \left[\Gamma \frac{\partial \Phi}{\partial x} \right] + \frac{\partial}{\partial y} \left[\Gamma \frac{\partial \Phi}{\partial y} \right] + \frac{\partial}{\partial z} \left[\Gamma \frac{\partial \Phi}{\partial z} \right]}_{\text{diffusion}} + \underbrace{S_\Phi}_{\text{source}} \quad (1)$$

Equation (1) is the so-called transport equation for the property Φ . It illustrates the various physical transport processes occurring in the fluid flow. The local acceleration and advection terms on the left-hand side are equivalent to the diffusion term ($\Gamma =$ diffusion coefficient) and the source term (S_Φ) on the right-hand side, respectively.

Table 1. Material property

Material	Density (kg/m ³)	Thermal conductivity (W/m K)	Specific heat (J/kg K)
Ceramic ware	2,300	1.5	1,004
Insulating Fiberbrick	1,140	0.53	1,000
Ceramic Fibre	200	0.44	1,130
Air	1.164	0.0263	1,007

In the simulation, the materials were used: Ceramic ware, Insulating Fiberbrick, Ceramic Fibre, Air, while fluid properties. The solid properties were defined by the user, as displayed in Table and the boundary conditions of the studied domain are presented in Table .

Table 2. Boundary conditions.

Description	Inlet 1	Inlet 2	Inlet 3	Inlet 4	outlet
Velocity (m/sec)	0.89	0.87	5	5	
Temperature (°C)	1200	27	27	27	
Turbulence intensity (%)	3	3	3	3	3
Hydraulic diameter (m)	0.085	0.01	0.006	0.024	0.24
Gauge Pressure (pascal)					0
Backflow Total Temperature (°C)					27

The inlet1 is mentioned as the burner port number 1 to 10. The inlet 2 is the gap between kiln car and kiln floor. The inlet 3 and inlet 4 are dilution air damper. The top wall, front (door) wall, the side wall and the rear wall are mentioned as ceramic fiber. The kiln car, the kiln floor and the chimney are mentioned as insulation fiberbrick. And the product and furniture are mentioned as ceramic ware.

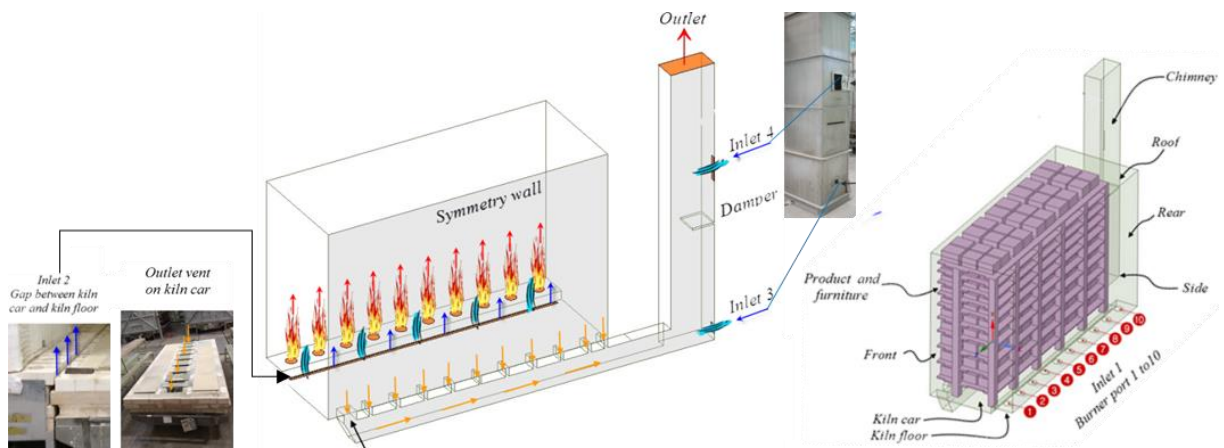


Figure 3. The position of inlet fluid, outlet fluid, burners and shelf inside kiln

CFD model shows the result of temperature and flow fields of fluid displayed on 3 planes along Y (0.18 m, 0.82 m and 1.42 m, be respectively high from the bottom) and 10 planes along Z axis (B1 – B10) as shown in Figure 4.

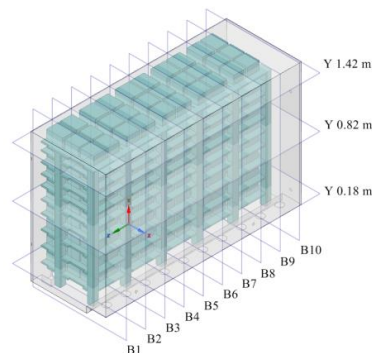


Figure 4. The plans used for displaying simulation results

3. Results and Discussion

3.1. Experimental results

According to the temperature of hot air at the above of burner in Figure 5(a), the temperature rises rapidly during the first 5 minutes and then it gradually increases according to time until firing process is finished. The maximum temperature is about 1200°C. In Figure 5(b), The temperature inside the kiln

collected from thermocouples shows the changing rate in the same direction. The temperature increases rapidly in the heating step at the rate of $0.08^{\circ}\text{C}/\text{sec}$. then, in the firing step, the increasing rate of temperature was $0.03^{\circ}\text{C}/\text{sec}$ until reaching to the maximum temperature, $\sim 1200^{\circ}\text{C}$. After that, soaking step, the highest temperature was controlled as constant for 30 minutes. During soaking step, the temperature distribution in this range varies about 67°C (6%) and the average temperature details presented in Figure 6(a). The temperature values at the 3 points of front middle and rear roofs were quite similar round $1,160^{\circ}\text{C}$. The temperature middle roof area presents minimal different temperature because it is the point used to control the sintering temperature. The wall door and rear door area display the lowest temperature because both were recorded at bottom kiln. Normally for this kiln kind, the temperature of the top is higher than the bottom. The side area shows the highest temperature around 1200°C because it's close to burner. All 6 positions have a standard deviation of 28°C . In the chimney, the average temperature and differential pressure is about 524°C and 28.4 pascal, respectively. The chimney provides lowest average temperature since there are 3 air inlets nearby it that are the gap between kiln car and kiln floor, inlet3 and inlet4 as shown in Figure 3.

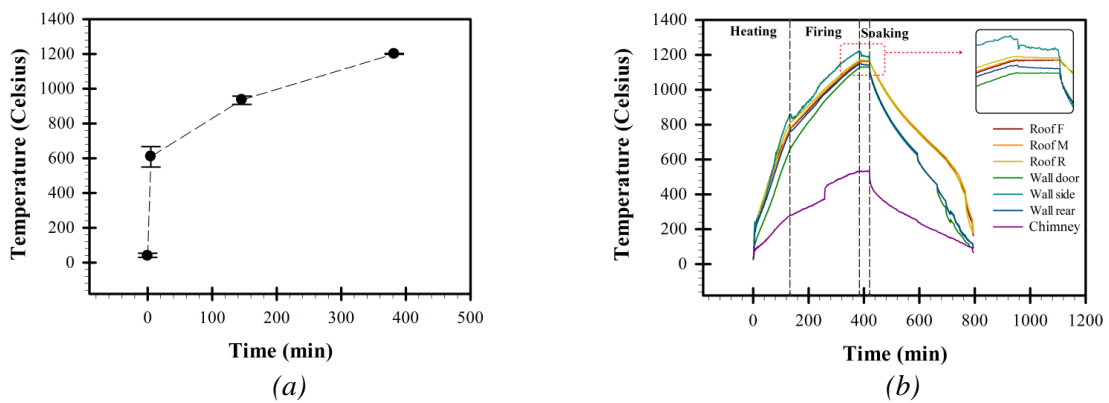


Figure 5. (a) Trend of measured temperature during firing processes; (b) Temperature inside the kiln

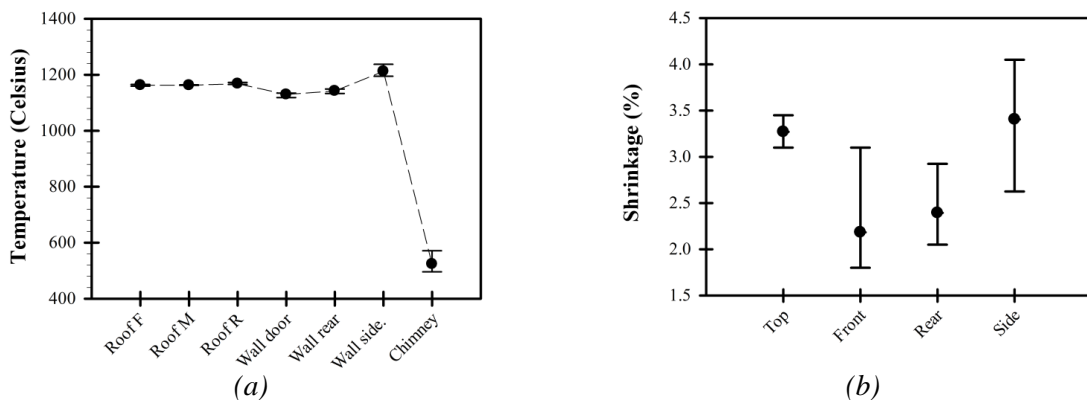


Figure 6. (a) Temperature distribution at soaking step; (b) Shrinkage of pyrometric device

When comparing the trend of temperature obtained from Figure 6(a) and the shrinkage of pyrometric device Figure 6(b), the top and side area in Figure 6(b) provides highest shrinkage. These areas are the same area of front, middle, rear roof and wall side. The highest shrinkage is equivalent to highest temperature. Moreover, the front and rear area in Figure 6(b) provides lower shrinkage. These are the same way of lower temperature at wall door and wall rear in Figure 6(a)

3.2. Numerical simulation results

Before the model was applied, the data of outlet gas flow rate and temperature in chimney as well as average kiln car temperature was used as representative to perform grid Independence analysis. Considering to Figure 7(a), the results were unstable when the number of grids was increased about 30% from beginning. They were insignificant changing when the number of grid cells was over 720,000. This

condition was used in this model. Figure 7(a) shows confirmation of insignificant changing the results between 721,901 and 6,532,566 grid cells.

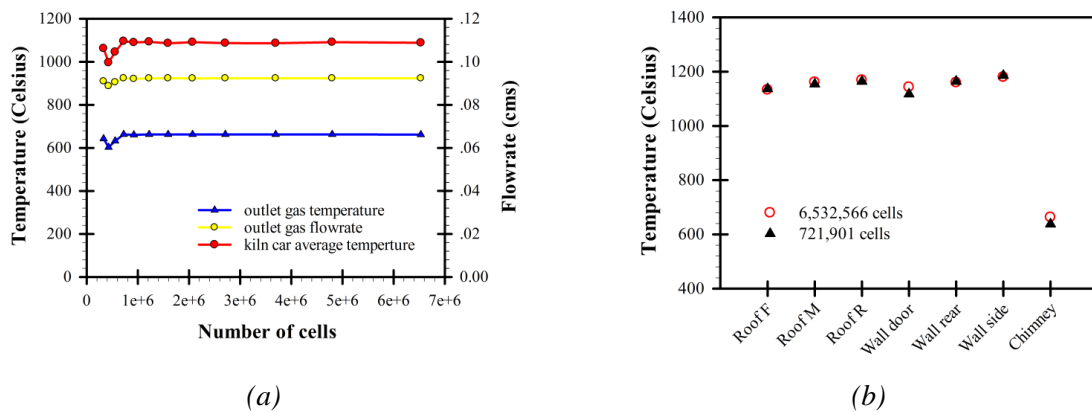


Figure 7. (a) Grid independence study results; (b) Comparison results of different grid cells

When comparing the temperature results from the model with these from experiment, they were the same trends as shown in Figure 8. The temperature results obtained from model were errored from these from experiment about -2 to 5% except the chimney, these error from experiment for 19.6%.

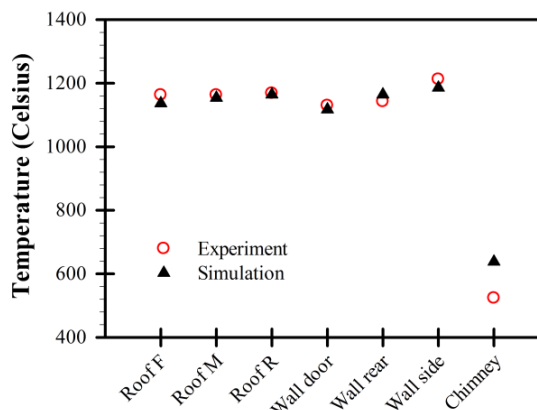


Figure 8. Temperature comparison results between model and actual measurement

Considering at level of 1.42 m along Y axis, the simulated temperatures at the 1st to 10th burner position (B1 – B10) was stable along X axis (area of center to wall side). The average different temperature at B1 – B10 was around 25 °C. The lowest and highest temperature presents at the front area (B1) and at the rear area (B10), respectively. At the Y level of 0.82 m, the temperature at 1st to 3rd burner positions (B1 – B3) was gradually decreases along X axis whereas the temperature at B4 – B10 was gradually increases along X axis. The highest temperatures occurred at B6 and B7 whereas the lowest temperature occurred at B1 and B2. The different temperature of B1 – B10 was 40 – 80 °C. The highest different temperature occurred at X position over 0.63 m. When focusing at lowest level along Y axis (0.18 m), the overall temperatures were significantly lower than these in higher level about 420 °C. The temperatures of B1 – B10 were decreased along middle kiln, X = 0 to X = 0.55 m. In this period, the different temperature between B1 – B10 was around 250 °C. At the position of X = 0.55 m to X = 0.75 m, overall temperatures were extremely increase since it's close to burner position. The different temperature of B1 – B10 at position of X = 0.55 was around 200 °C whereas that at position of X = 0.75 was around 60 °C. At the position over X = 0.75 m, overall temperatures were slightly decreased and the different temperature between B1 – B10 was around 180 °C. It was seen that the temperature distribution in Y level of 0.82 m was high fluctuation. This is the cause why should avoid placing workpieces in this area.

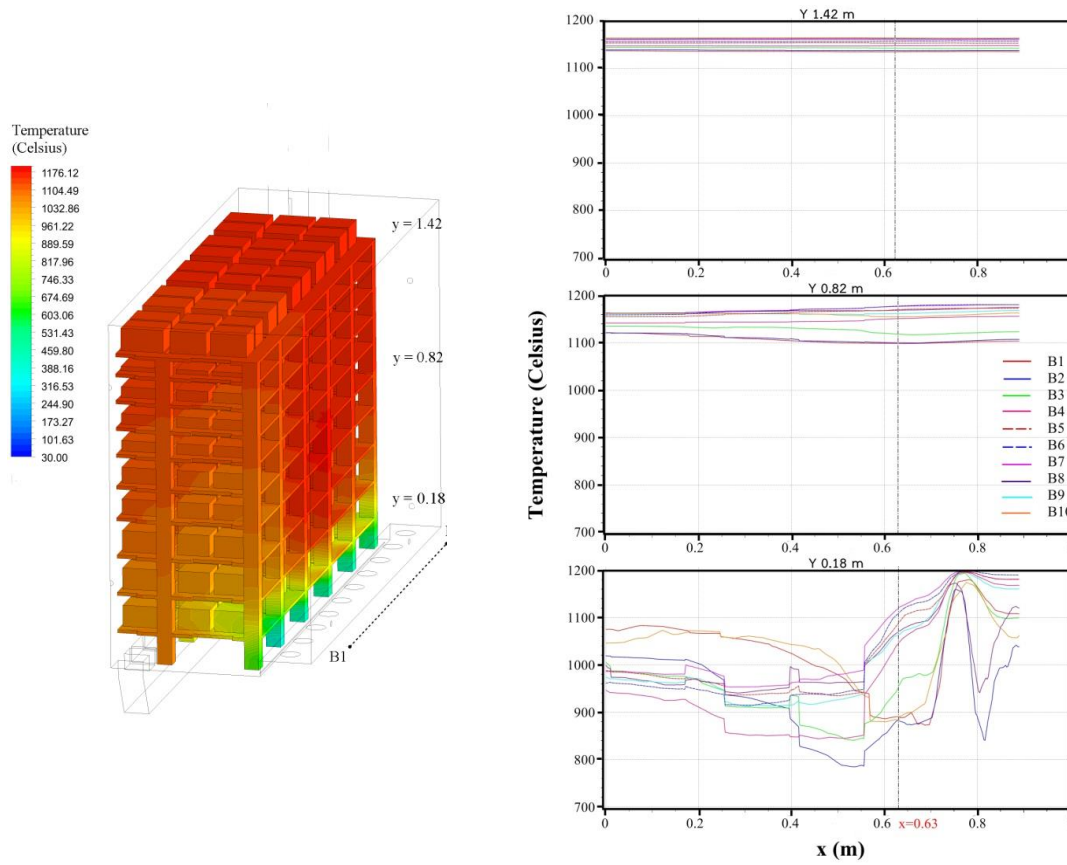


Figure 9. The simulated temperature of plane B1 – B10 along X axis in each different height along Y axis

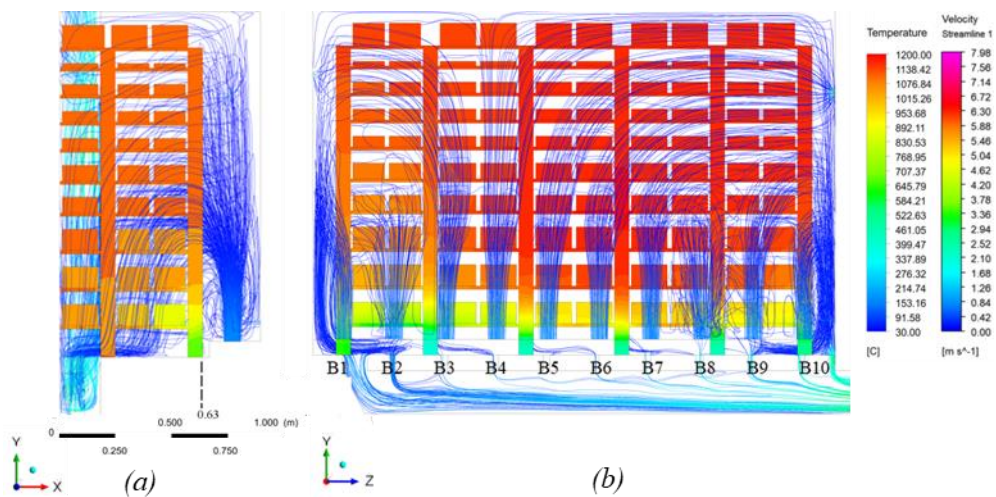


Figure 10. The airflow and temperature distribution inside the furnace:
(a) X-Y section of the front view ; (b) Z-Y section of the side view

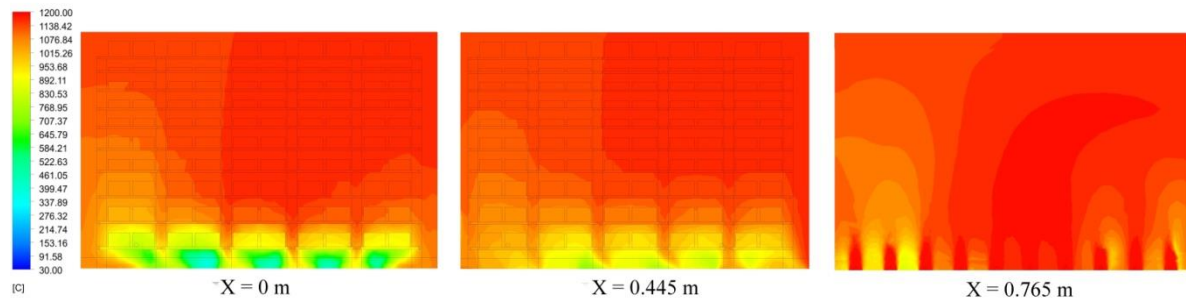


Figure 11. *Temperature contours at Y-Z plane*

Incident occurred in the kiln Figure 10(a) shows the hot air flowed from the burner to the ceiling then backed down through the gap of each shelf layers and workpiece. Finally, it leaved through the exit chimney. Considering Figure 10(b), the hot air steam lines from B1 – B3 slant towards the front kiln. Whereas, these from B4 – B10 flow to back kiln since the exhaust air existed at back kiln and near the chimney. This makes temperature at back kiln be higher than the front kiln Figure 11. Hot air flow should be balanced at both front and back kiln. This can improve better temperature distribution than conventional. When considering the 1st shelf level, it's low hot air stream line at this level leading to lower temperature compared to others. This should be significantly improved to

If we improve what is occurred, it will help the temperature of the lower layer tending to increase. The workpieces placed in this area will be ripen better.

4. Conclusions

The test result of the temperature distribution of the ceramic kiln during the soaking fire was used as a reference and comparison with the results of the CFD. The lowest temperature was about 850°C on the bottom level nearby the door and behind kiln. The highest temperature was about 1,200°C and occurred at the side wall near burner. At the roof area, temperature distribution was quite stable around 1,165°. All actual temperature measurement has a standard deviation of 28 °C. Its trend was also the same way with CFD results. The error between CFD and experiment results was -2% to 5%. Therefore, the model was utilized to predict and explain the phenomenon in the kiln. The CFD investigation come from 3 dimensions (X, Y, Z). Along Y axis (height), the are 3 planes located in different shelves levels while along Z axis (depth), the are 10 planes at the burner location. The temperature at the top level (kiln roof) was uniform and stable. And the temperature fluctuation was about 25 °C. At the middle height level, temperature at the front kiln was slightly lower than the that back kiln. Because there is a dense amount of hot air from the 4th to 10th burner that is higher than from 1st to 3rd burner. At the lowest levels, there is high fluctuation of temperature around 500°C occurring from 1st to 10th burner. When considering along X axis (width), The maximum temperature was 1200°C at the burner position (X = 0.75m). At the center of the kiln (X = 0), temperature was about 800 °C. And at the position of X = 0.55m, lowest temperature around 790°C was occurred. This volatility temperature distribution in this level result in avoiding workpieces installation. Therefore, temperature balance and management should be done in the bottom kiln area.

Acknowledgments

The author really highly appreciated for all kind supports, facilities and CFD software from Rajamangala University of Technology Lanna and Chiang Mai University. Furthermore, the author is sincerely grateful for the support of Indra Ceramic Factory who allows to use all tools and machines for study and development.

REFERENCES

- [1] F. Norton, *Ceramics for the Artist Potter*. Cambridge, MA: Addison, ed: Wesley Publishing Co., Inc, 1956.
- [2] T. Fongsamootr and N. Doungsupa, "Simulation of Combustion in Ceramic Fiber Kiln using Computational Fluid Dynamics," *WSEAS Transactions on Fluid Mechanics*, vol. 1, no. 1, p. 16, 2006.
- [3] T. S. Possamai, R. Oba, V. Nicolau, and O. Otte, "Numerical simulation of a ceramic kiln used in frits production," in *20th International Congress of Mechanical Engineering, Gramado, RS, Brazil COB09*, 2009, vol. 1152.
- [4] Z. Zhang, J. Feng, and W. Liu, "Firing Simulation Studies of Household Porcelain in Shuttle Kilns," in *International Conference on Computer Information Systems and Industrial Applications*, 2015: Atlantis Press, pp. 804-807.

- [5] K. Krumov and N. Penkova, "Numerical analysis of the transient heat transfer in high temperature chamber furnaces," in *IOP Conference Series: Materials Science and Engineering*, 2019, vol. 595, no. 1: IOP Publishing, p. 012005.
- [6] K. S. Krumov and N. Y. Penkova, "Improvement of the Conjugate Heat Transfer in High Temperature Chamber Furnaces for Firing of Ceramic Ware," *Journal of Civil Engineering and Architecture*, vol. 13, pp. 265-272, 2019.
- [7] M. Romero-Flores, A. D. Tapia-Martínez, K. Mariella-González, A. Cantú-Pérez, and A. Montesinos-Castellanos, "Temperature uniformity evaluation of a shuttle kiln for the sanitary ware industry using CFD," (in EN), *Combustion Theory and Modelling*, vol. 24, no. 6, pp. 1070-1089, 2020.
- [8] U. Adhikari, B. Prajapati, and A. M. Bhandari, "Performance evaluation and thermal analysis of pottery furnace in Thimi, Bhaktapur," *Journal of Innovations in Engineering Education*, vol. 4, no. 2, pp. 128-137, 2021.
- [9] L. Punsukmtana *et al.*, "A comparative study of the firing shrinkage properties of the process temperature control rings," (in TH), *Bulletin of Applied Sciences*, vol. 03, no.3, p. 9, 2014.
- [10] H. Danninger, Ch. Xu, Ch. Gierl, A. Avakemian, and M.-Ch. Huemer, "In-Situ Characterization of The Sintering Process Through Process-Temperature Control Rings.," (in EN), *Powder Metallurgy Progress*, internet vol. 12, 3, pp. 168-180, 2012. [Online]. Available: http://www.imr.saske.sk/pmp/c03_2012.html.
- [11] S. Ferrer, A. Mezquita, M. P. Gómez-Tena, C. Machí, and E. Monfort, "Estimation of the heat of reaction in traditional ceramic compositions," *Applied Clay Science*, vol. 108, pp. 28-39, 2015.
- [12] F. Smith, D. Wagoner, and A. Nelson, "Guidelines for Development of a Quality Assurance Program: Volume I. Determination of Stack Gas Velocity and Volumetric Flow Rate(Type-S Pitot Tube)," 1974.
- [13] J. Tu, G. H. Yeoh, and C. Liu, *Computational Fluid Dynamics A Practical Approach*. Oxford ,UK: Elsevier (in EN), 2008.
- [14] W. L. McCabe, J. C. Smith, and P. Harriott, *Unit operations of chemical engineering*. McGraw-hill New York, 1993.
- [15] JIS C series Insulating Firebrick, Japan, 2016. [Online]. Available: https://www.isolite.co.jp/en/products/taika/c_insulation/.



Chartchai Dechpratoom received the B.S. Tech.Ed. degree in Mechanical Engineering from the Rajamangala Institute of Technology, Bangkok, Thailand in 1997. From 2005 to present, he has worked as Engineering Manager at the INDRA CERAMIC Co.Ltd. Lampang Thailand. His research interest includes the carbon reduction in ceramic industrial, process improvement, energy management system. Email: d_chartchai@hotmail.com



Arpiruk Hokpunna received his doctorate in Engineering from the Technical University of Munich, Germany, in 2009. He is currently an assistant professor at Chiang Mai University, Thailand. His research field includes numerical methods for fluid flow, industrial modeling, simulation and design as well precision agriculture. Email: a.hokpunna@bv.tum.de



Pracha Yeunyongkul received his D.Eng. in Mechanical engineering from ChiangMai University, Thailand, in 2012. He is currently an assistant professor at Rajamangala University of Technology Lanna, Thailand. His research interests include application of heat pipe, heat exchanger design and geopolymer. Email: ypracha@rmutl.ac.th



Ronnachart Munsin is working as an assistant professor at RMUTL. He received his D.Eng. in Mechanical Engineering from KMUTT, Thailand, in 2015 and worked as a postdoctoral fellow at the Université d'Orléans, France, in 2016. His research focuses on atmospheric water harvesting, agricultural engineering and combustion. Email: ronnachart@rmutl.ac.th



Thanawat Watcharadumrongsak is working as an instructor at Rajamangala University of Technology Lanna, Thailand. He received doctor degree in Mechanical Engineering from Chiang Mai University, Thailand. His research focuses on heat transfer and applications. Email: thanachak@rmutl.ac.th



Korawat Wuttikid is working as an instructor at Rajamangala University of Technology Lanna. He received bachelor, master and doctor degree in Mechanical Engineering from Chiang Mai University. His research focus on machine design and energy management for solving engineering problem in industry. Email: kor_wat@hotmail.com